


Icaritin alleviates docetaxel-induced skin injury by suppressing reactive oxygen species via estrogen receptors

Jie Zou¹ | Meng-Xia Xu¹ | Fang Li² | Yu-Hao Wang¹ | Xiao-Qian Li¹ |
 Dao-Jiang Yu³ | Yi-Jia Ma¹ | Yuan-Yuan Zhang¹  | Xiao-Dong Sun¹

¹West China School of Basic Medical Sciences & Forensic Medicine, Sichuan University, Chengdu, China

²Department of Hepatopancreatobiliary Surgery, Sichuan Cancer Hospital and Institute, School of Medicine, University of Electronic Science and Technology of China, Chengdu, China

³Department of Plastic Surgery, The Second Affiliated Hospital of Chengdu Medical College, China National Nuclear Corporation 416 Hospital, Chengdu, China

Correspondence

Yuan-Yuan Zhang and Xiao-Dong Sun, West China School of Basic Medical Sciences & Forensic Medicine, Sichuan University, Chengdu, 610041, China.

Email: zhangyy@scu.edu.cn, sarahyyzhang@hotmail.com and sunxdelta@hotmail.com

Funding information

the Sichuan Provincial Key Laboratory of Radiation Oncology, Grant/Award Number: 2020FSZLX-02; National Natural Science Foundation of China, Grant/Award Numbers: 81770580, 82170844

Abstract

Background: Docetaxel (DTX) exhibits antitumor effects against breast cancer by stabilizing microtubules and increasing the accumulation of reactive oxygen species (ROS). DTX extravasation during infusion often causes skin injury. The present study aimed to investigate the effects and mechanisms of icaritin (ICT) on DTX-induced skin injury.

Methods: The effects of ICT on the viability and apoptosis of HaCaT cells were measured by SRB assay and flow cytometry, respectively. Endogenous LC3 puncta and microtubules were determined by immunofluorescence. The number of mitochondria was measured by MitoTracker orange staining. ROS were determined by dihydroethidium staining. The expression of markers of ROS and autophagy were measured by western blotting. Chloroquine, compound D, and tamoxifen were employed as the inhibitor for autophagy and AMPK, estrogen receptors (ERs) modulator, respectively.

Results: DTX inhibited the viability and decreased apoptosis of HaCaT cells, which can be rescued by ICT. ICT decreased microtubule bundles, increased the number of mitochondria, and attenuated ROS of HaCaT cells induced by DTX. ICT blocks autophagy and the autophagic flux. Compound C or tamoxifen diminished the protection effects of ICT on DTX-treated HaCaT cells.

Conclusion: ICT alleviates DTX-induced skin injury by suppressing ROS, reducing microtubule bundles, and blocking autophagy via ERs. Our study indicated that ICT may be a potential candidate for DTX-induced skin injury.

KEYWORDS

autophagy, docetaxel, estrogen receptors, icaritin, skin injury

INTRODUCTION

Docetaxel (DTX), a semisynthetic derivative of paclitaxel, is a water-soluble compound of the natural precursor 10-deacetylbaobacatin III isolated from *Taxus baccata*.¹ DTX plays antitumor effects through the same mechanism as paclitaxel which promotes the microtubule bundles.² DTX is intravenously administered in clinical application and widely used for many cancers, especially breast cancer.³

During the infusion process, DTX extravasation often causes skin injury. There are no specific pharmacological agents or recommended treatments for DTX extravasation in guidelines. Most cases reported that conservative treatments were used for DTX extravasation-induced skin injury. Some cases were treated with glycerol, hyaluronidase, and other topical treatments, while these treatments achieved poor effects.⁴

Mitochondrial dysfunction is one of the hallmarks of many cancers.⁵ Mitochondrial dysfunction not only mediates tumor cell metastasis but also affects the overall level of cell metabolism and changes cell morphology since

Jie Zou, Meng-Xia Xu, and Fang Li contributed equally to this work.

This is an open access article under the terms of the Creative Commons Attribution-NonCommercial-NoDerivs License, which permits use and distribution in any medium, provided the original work is properly cited, the use is non-commercial and no modifications or adaptations are made.

© 2021 The Authors. *Thoracic Cancer* published by China Lung Oncology Group and John Wiley & Sons Australia, Ltd.

mitochondrial metabolism is at the center of metabolic integration.⁶ Interestingly, a large number of studies have demonstrated that mitochondrial dysfunction is closely related to skin injury. Mitochondrial dysfunction promotes tumor formation⁷ and accelerates skin aging and death⁸ by producing too many reactive oxygen species (ROS). Excessive accumulation of ROS disrupts cell balance, leads to mitochondrial dysfunction, and induces autophagy at the same time. In turn, autophagy helps to reduce oxidative damage and degrade oxidized substances to downregulate ROS.⁹ One of the main mechanisms for maintaining cell balance is to remove damaged mitochondria and excessive ROS by upregulating autophagy. Autophagy is promoted by the serine/threonine kinase adenosine 5'-monophosphate (AMP)-activated protein kinase (AMPK).¹⁰ Importantly, AMPK is a key target of cells in response to energy stress and mitochondrial damage, which coordinates various features of autophagy and mitochondrial biology.¹¹

Icaritin (ICT, 3,5,7-trihydroxy-2-(4-methoxyphenyl)-8-(3-methylbut-2-enyl)chromen-4-one) is one of the main metabolites of icariin.¹² ICT has been reported to alleviate osteoporosis in ovariectomized female mice, indicating that ICT has an estrogen-like effect.¹³ Other than that, our previous study demonstrated that the antitumor effects of ICT against breast cancer depended on the status of estrogen receptors (ER).¹⁴ ICT was reported to act as an upstream molecule of autophagy to activate AMPK in colorectal cancer cells.¹⁵ We therefore hypothesized that ICT alleviates DTX-induced skin injury by regulating autophagy and ROS through activating AMPK via ER.

In this study, we aimed to investigate the effects and mechanisms of ICT on DTX-induced skin injury. HaCaT cells were induced with DTX (2.5 nM) for 48 h to establish the cell model. The autophagy markers and ROS levels were measured by western blotting and immunofluorescence. Chloroquine (CQ), compound C (CoC), and tamoxifen (TAM) were employed as the inhibitor for autophagy, AMPK, and ER, respectively.

METHODS

Cell culture

Dulbecco's Modified Eagle Medium (DMEM) high glucose medium and penicillin-streptomycin (PS) were obtained from HyClone. Fetal bovine serum (FBS) was acquired from Biological Industries. HaCaT cells were a kind gift from Professor Shuyu Zhang of Sichuan University and cultured in DMEM high glucose medium supplemented with 10% FBS and 1% PS. All cells were maintained at 37°C in a humidified atmosphere containing 5% CO₂. HaCaT cells were induced with DTX (2.5 nM) for 48 h and then treated with ICT (10 μM) alone, or in combination with CQ (10 μM), CoC (10 μM), or TAM (15 μM) for 24 h, respectively.

Cell viability assay

The method of sulforhodamine B (SRB) colorimetric assay was improved based on the method of Vanicha Vichai.¹⁶ Precooled 10% trichloroacetic acid (TCA, Kelong) solution was added to cells for fixation at 4°C for 1 h. Cells were washed with double-distilled water (ddH₂O) and air dried. Then, 0.4% SRB (Sigma) solution was added to cells for staining for 10 min. Float color was washed with 1% glacial acetic acid solution and then aired. Then, 10 mM Tris-base (BBI Life Sciences) solution was added and absorbance was measured at 510 nm with a microplate meter (Thermo Fisher Scientific, Inc.). The viability of cells was calculated as follows: %cell viability = $\frac{OD_{drug} - OD_{blank}}{OD_{control} - OD_{blank}} \times 100\%$. Median inhibition concentration (IC₅₀) values were estimated using nonlinear regression models as follows: $Y = Bottom + \frac{Top - Bottom}{1 + 10^{X - LogIC50}}$.

Flow cytometry

The apoptotic cells were quantified using the annexin V-FITC apoptosis detection kit (Beyotime) according to the manufacturer's instructions.¹⁷ Cells were digested, collected by centrifugation at 800 rpm for 3 min, washed with phosphate-buffered saline (PBS), and resuspended in annexin V-FITC binding buffer. Cells were then transferred to a flow tube, incubated with 5 μl annexin V-FITC and 10 μl propidium iodide (PI) for 20 min in the darkness. The samples were immediately analyzed using flow cytometry (BD Biosciences) in the FITC and PE channel. Data acquisition and analysis were performed using FACSDiva and FlowJo software (BD Biosciences).

Immunofluorescence

Endogenous microtubule-associated protein 1A/1B-light chain 3 (LC3) was determined by immunofluorescence as follows.¹⁸ Cells were washed twice with PBS and fixed with 4% paraformaldehyde (PFA, Sangon Bio-Tech) for 20 min at room temperature (RT). Afterward, cells were incubated with 0.5% TritonX-100 (BBI Life Sciences) for 15 min and blocked by 4% albumin from bovine serum (BSA, Sangon Bio-Tech) for 1 h at RT. Cells were then incubated with the primary antibody, anti-LC3 antibody (Medical & Biological Laboratories), at RT for 2 h. After being washed twice with PBS, cells were incubated with the secondary antibody, fluorescent FITC-conjugated antibody (Thermo Fisher Scientific) for 1 h in the darkness at RT. Nuclei were stained with Hoechst 33258 (Sigma) for 3 min at RT. Cells were washed with PBS 3 times and sealed by an antifluorescence quenching agent. Images were captured under a Zeiss LSM 710 confocal microscope.

Microtubules were determined by immunofluorescence as follows.¹⁹ Cells were fixed with methanol for 5 min at -20°C and incubated with PBS for 5 min at RT. Cells were

then blocked by 4% BSA (Sangon Bio-Tech) for 1 h at RT and incubated with the primary antibody against α -tubulin (Santa Cruz) for 2 h at RT. After being washed twice with PBS, cells were incubated with the secondary antibody, fluorescent FITC-conjugated antibody (Thermo Fisher Scientific, Inc.) for 1 h in the darkness at RT. Nuclei were stained with Hoechst 33258 (Sigma) for 3 min at RT. Cells were washed three times with PBS and sealed by an anti-fluorescence quenching agent. Images were captured under Zeiss LSM 710 confocal microscope.

Western blotting

Cell lysates were subjected to western blotting and total protein extracts were obtained as previously described.²⁰ Equivalent amounts of proteins were loaded into sodium dodecyl sulfate-polyacrylamide gel electrophoresis (SDS-PAGE) and electrophoretic at 100 V for 1.5 h. Proteins were then transferred to the polyvinylidene fluoride (PVDF) membrane. Membranes were then incubated with the primary antibodies at 4°C overnight, washed with the Tris-buffered saline with 0.1% Tween 20 detergent (TBST) three times, and incubated with the secondary antibodies conjugated to horseradish peroxidase (Invitrogen) for 1 h at RT. Chemiluminescence images were acquired by darkroom development. Antibodies against superoxide dismutase type 1 (SOD1), superoxide dismutase type 2 (SOD2), AMPK α subunit (AMPK α), autophagy-related 5 (ATG5), ER α , glyceraldehyde 3-phosphate dehydrogenase (GAPDH) were obtained from Proteintech. The antibody against phosphor-AMPK α (p-AMPK α) was obtained from Cell Signaling Biotechnology. Antibodies against NAD(P)H: quinone oxidoreductase (NQO1) and autophagy-related 7 (ATG7) were obtained from Sangon Biotech. Antibodies against microtubule-associated protein 1A/1B-light chain 3 (LC3) and the ubiquitin-binding autophagy receptor protein (p62) were acquired from Medical & Biological Laboratories.

MitoTracker staining

The number of mitochondria was detected by MitoTracker staining as previously described.²¹ Cells were washed with PBS twice and incubated with MitoTracker orange probe (Invitrogen) (300 nM) for 20 min at 37°C in a humidified atmosphere. Cells were then washed three times with PBS, fixed by 4% PFA (Sangon Bio-Tech) for 15 min, and permeated by 0.5% TritonX-100 (BBI) for 15–20 min. Nuclei were stained by Hoechst 33258 (Sigma) for 3 min. Images were analyzed with ImageJ software (National Institute of Health [NIH], USA).

Dihydroethidium (DHE) staining

Cells were digested and collected by centrifugation at 800 rpm for 3 min. Cells were then resuspended in warm

PBS and centrifuged at 800 rpm for 3 min before being incubated with DHE solution (7.5 μ M) for 30 min in the dark. Cells were centrifuged at 800 rpm for 3 min, resuspended, and washed with PBS three times. Then cells were resuspended with PBS, transferred to a flow tube, and measured on the flow cytometer (BD Biosciences) in the FITC channel. Data acquisition and analysis were performed using FACSDiva and FlowJo software (BD Biosciences).

Statistical analysis

All experiments were performed in triplicate and all data are expressed as the mean \pm standard deviation (SD). All data were analyzed by one-way ANOVA using Graph-Pad Prism 8.4.3 software. *p*-values less than 0.05 were considered statistically significant.

RESULTS

ICT enhances the viability and reduces apoptosis of DTX-induced HaCaT cells

Our previous study reported that ICT shows the optimal inhibition effect on breast cancer cells at 10 μ M.¹⁴ Therefore, a concentration of 10 μ M of ICT was employed in the present study. As shown in Figure 1a, the IC₅₀ of DTX is 2.373 nM without ICT and 5.222 nM with ICT, respectively. ICT significantly enhances the viability of DTX-induced HaCaT cells at 0.6, 1.2, 2.5, 5, 10, 20, 40, and 80 μ M (Figure 1b). ICT rescues the necrosis and inhibits late apoptosis of DTX-induced HaCaT cells (Figure 1c,d). These results indicated that ICT promotes cell viability by reducing the necrosis and late apoptosis of DTX-induced HaCaT cells.

ICT alleviates the microtubule bundles in DTX-induced HaCaT cells

As shown in Figure 2a,b, DTX induced obvious microtubule bundles and nuclei damage of HaCaT cells, which was significantly alleviated by ICT. ICT remarkably increased the percentage of the normal nucleus. There is controversial evidence about the roles of tubule acetylation in the stability of microtubules. Some studies have suggested that tubulin acetylation enhances the stability of the microtubule,²² whereas, some reported that tubulin acetylation occurs only in stable microtubules rather than dynamic microtubules, indicating that acetylation itself cannot stabilize microtubules.²³ Nonetheless, both viewpoints support that tubulin acetylation is an important marker of the stability of microtubules. Therefore, we determined the expression of α -tubulin and acetylated- α -tubulin in DTX-induced HaCaT cells. As shown in Figure 2c,d, ICT reduced DTX-induced α -tubulin acetylation in HaCaT cells, indicating that ICT promotes the depolymerization of microtubules in HaCaT cells.

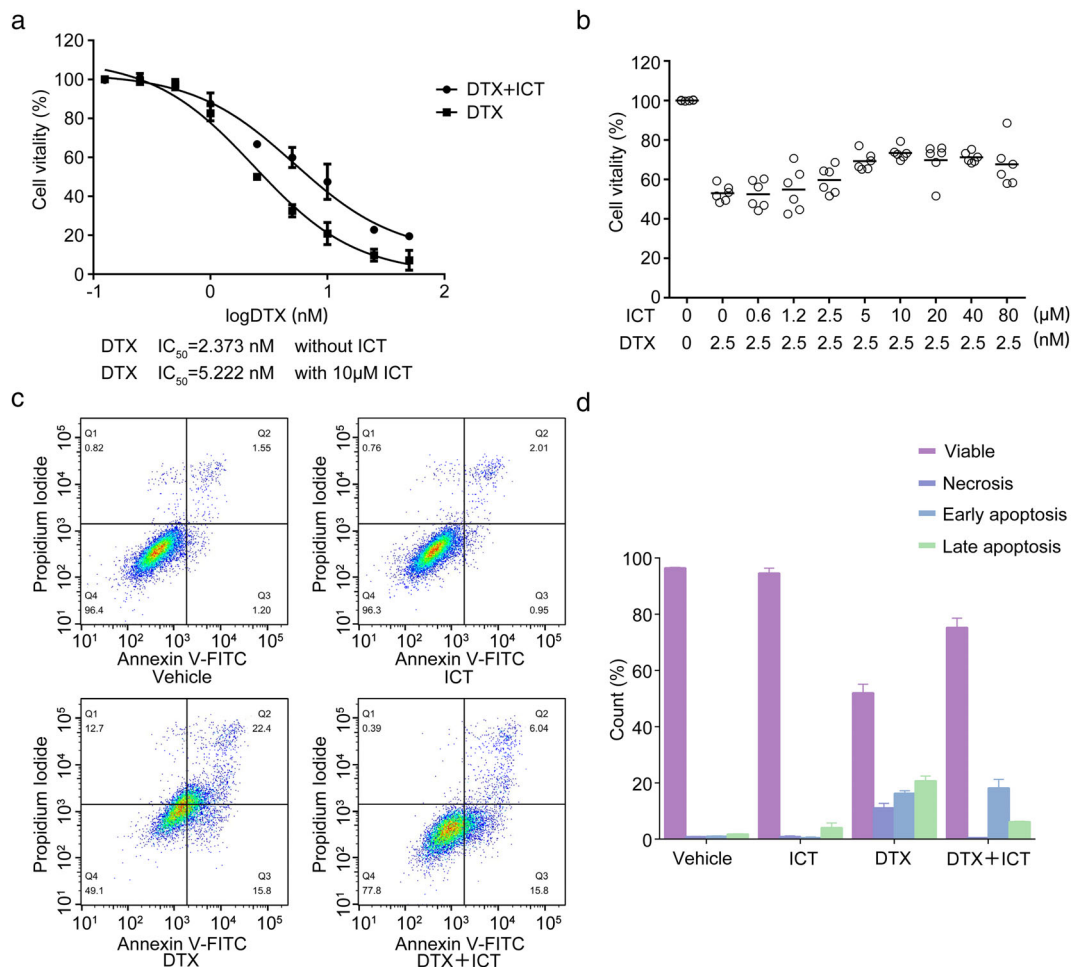


FIGURE 1 ICT increases viability and decreases apoptosis of HaCaT cells induced by DTX. HaCaT cells were induced with DTX for 48 h and then treated with ICT for 24 h. (a, b) Cell viability was detected by SRB assay. The cell viability was calculated by the following equation: $\% \text{cell viability} = \frac{OD_{\text{Drug}} - OD_{\text{blank}}}{OD_{\text{control}} - OD_{\text{blank}}} \times 100\%$. Median inhibitory concentration (IC_{50}) of the cell activity was estimated using nonlinear regression models by the following equation: $Y = \text{Bottom} + \frac{\text{Top} - \text{Bottom}}{1 + 10^{-(X - \text{LogIC}_{50})}}$. (c, d) The apoptosis of HaCaT cells was detected by flow cytometry after Annexin V and propidium iodide staining. All data were expressed as the mean \pm SD from three independent experiments. ICT, icaritin; DTX, docetaxel; SRB, sulforhodamine B; IC_{50} , median inhibition concentration

ICT increases the number of mitochondria and reduces ROS levels in DTX-induced HaCaT cells

As detected by MitoTracker staining, DTX decreased the number of mitochondria and induced nuclei damage, which was rescued by ICT (Figure 3a–c). Consistently, ICT reduced DTX-induced ROS levels in HaCaT cells (Figure 3d,e). The expression of antioxidant enzymes, SOD1, SOD2, and NQO1 was increased by ICT in HaCaT cells without DTX (Figure 3f–i). Interestingly, DTX also increased the expression of these antioxidant enzymes. However, ICT restored the increase of NQO1 in DTX-induced HaCaT cells, while ICT had no significant effects on the expression of SOD1 and SOD2 (Figure 3f–i). Although ICT leads to different trends of these antioxidant enzymes, ICT does increase their expression compared to normal cells. These results indicated that ICT increases the expression of antioxidant enzymes to reduce cellular ROS

levels in HaCaT cells. However, DTX causes excessive production and accumulation of ROS in HaCaT cells. Therefore cells have to express a large number of antioxidant enzymes to eliminate excessive ROS. In general, ICT eliminates cellular ROS by increasing the expression of antioxidant enzymes.

ICT reduces autophagy in HaCaT cells exposed to docetaxel

As shown in Figure 4a,b, ICT increased endogenous LC3 puncta in HaCaT cells, but not in DTX-induced HaCaT cells. Consistently, ICT increased the ratio of LC3-II/LC3-I in HaCaT cells, but not in DTX-induced HaCaT cells (Figure 4c,e). DTX increased the expression of p62 which was further increased by ICT (Figure 4c,d). These results indicated that although DTX promotes the production of

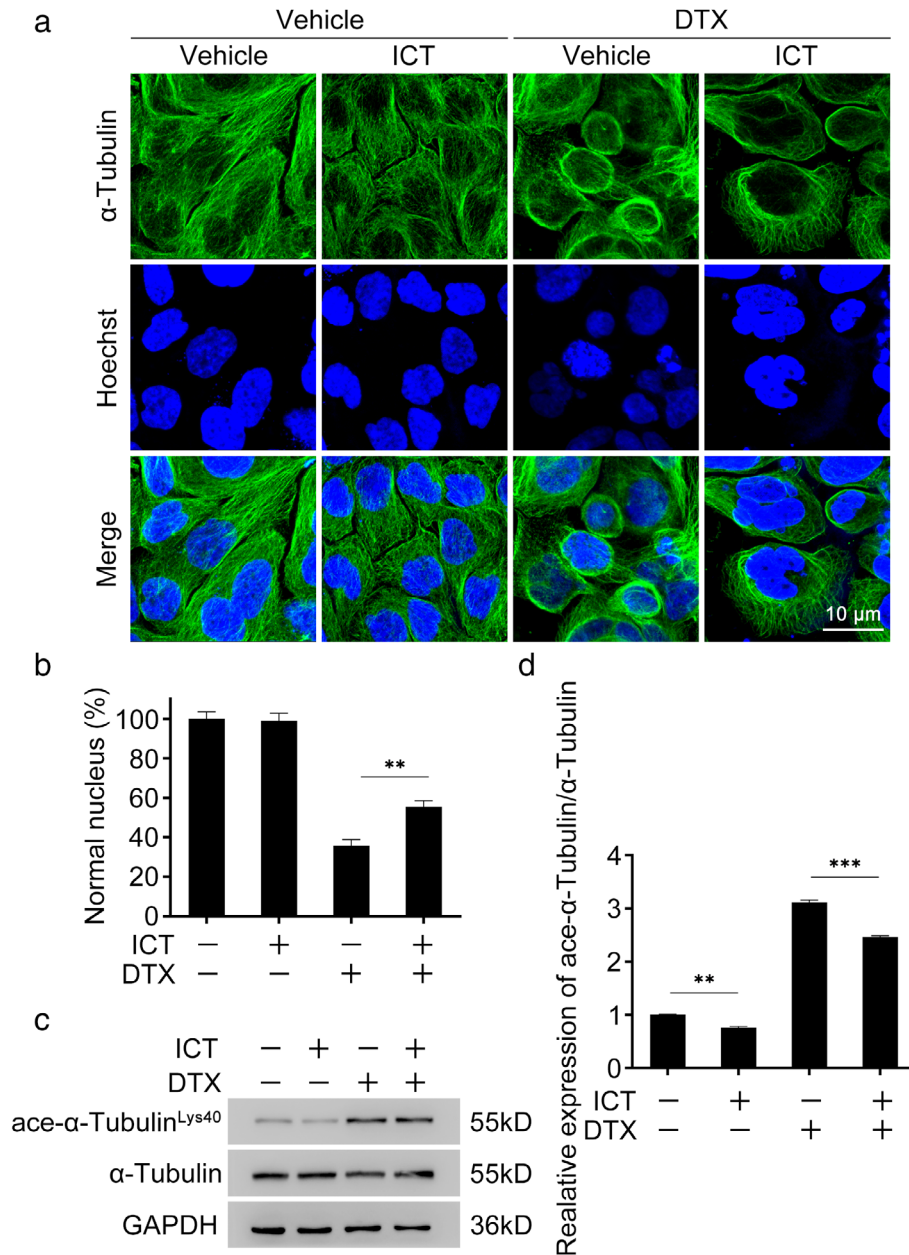


FIGURE 2 ICT reduces microtubule bundles in HaCaT cells induced by DTX. HaCaT cells were induced with DTX (2.5 nM) for 48 h and then treated with ICT (10 μ M) for 24 h. (a, b) The microtubule (green) and nucleus (blue) of HaCaT cells were detected by immunofluorescence and captured under confocal microscopy (scale bars = 10 μ m). The percentage of the normal nucleus was calculated by the following equation: $\% \text{normal nucleus} = \frac{\text{Total nucleus number} - \text{Abnormal nucleus number}}{\text{Total nucleus number}} \times 100\%$. (c, d) The expression of acetyl- α -tubulin and α -tubulin in HaCaT cells was measured by western blotting. The relative ratio of acetyl- α -tubulin/ α -tubulin was quantified. All data were expressed as the mean \pm SD from three independent experiments. *** $p < 0.001$; ** $p < 0.01$. ICT, icaritin; DTX, docetaxel; GAPDH, glyceraldehyde 3-phosphate dehydrogenase

autophagosomes, it inhibits the fusion of autophagosomes and lysosomes, that is, blocks the flow of autophagy. To elucidate the effects of ICT on the autophagic flux, we detected the expression of autophagy initiation proteins ATG5 and ATG7 in HaCaT cells. Both DTX and ICT increased the expression of ATG5 and ATG7 in HaCaT cells. It is worth noting that ICT decreased them in DTX-induced HaCaT cells (Figures 3f and 5a). CQ, a lysosome inhibitor, inhibits

the fusion of autophagosomes and lysosomes, thereby preventing the autophagic flux. As shown in Figure 5b,c, ICT decreased the LC3 puncta induced by DTX, which was reversed by CQ. CQ increased the expression of p62 and the ratio of LC3-II/LC3-I in DTX-induced HaCaT cells (Figure 5d-f). Our results proved that DTX activates the initiation of autophagy and blocks the flow of autophagy, while ICT directly blocks the entire autophagy.

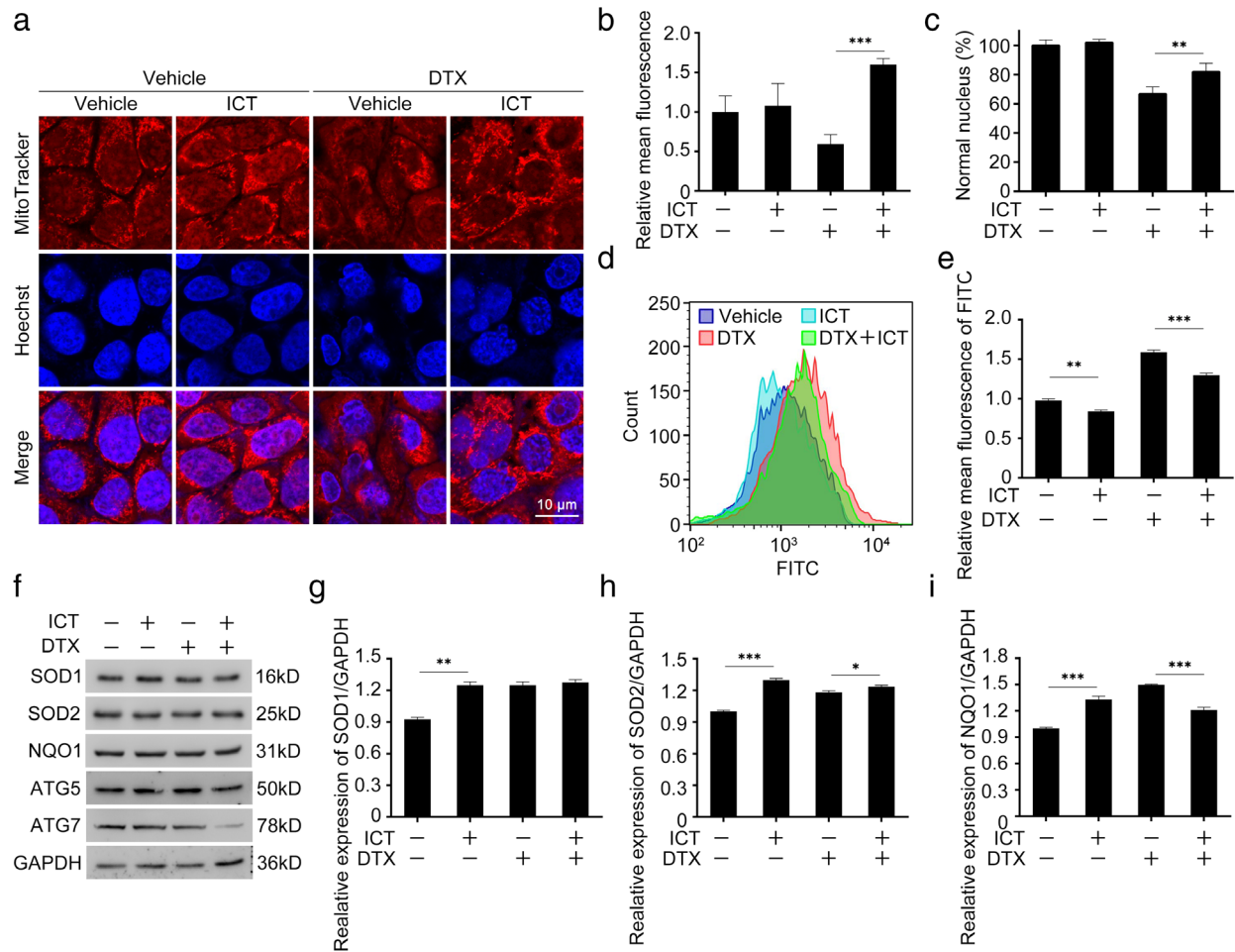


FIGURE 3 ICT increases the number of mitochondria and decreases ROS levels of HaCaT cells induced by DTX. HaCaT cells were induced with DTX (2.5 nM) for 48 h and then treated with ICT (10 μ M) for 24 h. (a–c) The mitochondria (red) and nucleus (blue) of HaCaT cells were detected by mitotracker staining (scale bars = 10 μ m). The percentage of the normal nucleus was calculated by the following equation: %normal nucleus = $\frac{\text{Total nucleus number} - \text{Abnormal nucleus number}}{\text{Total nucleus number}} \times 100\%$. (d, e) The levels of ROS of HaCaT cells were detected by flow cytometry (FITC channel) after DHE staining. (f, g) The expression of SOD1, SOD2, NQO1, ATG5, and ATG7 of HaCaT cells was detected by western blotting. The relative ratio of SOD1/GAPDH, SOD2/GAPDH, and NQO1/GAPDH was quantified. All data were expressed as the mean \pm SD from three independent experiments. *** $p < 0.001$; ** $p < 0.01$; * $p < 0.05$. ICT, icaritin; DTX, docetaxel; ROS, reactive oxygen species; DHE, dihydroethidium; SOD1, superoxide dismutase type 1; SOD2, superoxide dismutase type 2; NQO1, NAD(P)H: quinone oxidoreductase; GAPDH, glyceraldehyde 3-phosphate dehydrogenase

ICT regulates autophagy and ROS levels by activating AMPK in DTX-induced HaCaT cells

To confirm that ICT regulates autophagy through AMPK, the AMPK inhibitor, CoC, was employed to inhibit the phosphorylation of AMPK. As shown in Figure 6a,b, CoC blocked the effects of ICT on LC3 puncta. As detected by western blotting, ICT inhibits the phosphorylation of AMPK, which was further decreased by CoC (Figure 6f,h). Studies have shown that CoC activates cytoprotective autophagy through the AMPK-independent pathway²⁴ or inhibits autophagy by inhibiting AMPK.²⁵ Our results indicated that ICT regulated the level of autophagy by regulating AMPK to avoid programmed cell death (Figure 6a–f). In terms of oxidative stress, ICT down-regulated the expression of SOD1 and SOD2 in DTX-induced HaCaT cells in

combination with CoC (Figure 6c,g,h). These results showed that ICT regulates ROS through AMPK-independent pathways.

ICT regulates autophagy and ROS levels via ER in DTX-induced HaCaT cells

To elucidate the mechanisms of ICT, the estrogen receptor modulator, TAM, was employed. ICT increased the LC3 puncta in DTX-induced HaCaT cells, which was further increased by TAM (Figure 7a,b). ICT increased the phosphorylation of AMPK in DTX-induced HaCaT cells, which was reversed by TAM (Figure 7c,f). ICT reduced the flow of autophagy in DTX-induced HaCaT cells, which was blocked by TAM (Figure 7a–h). As shown in Figure 7i–k, ICT

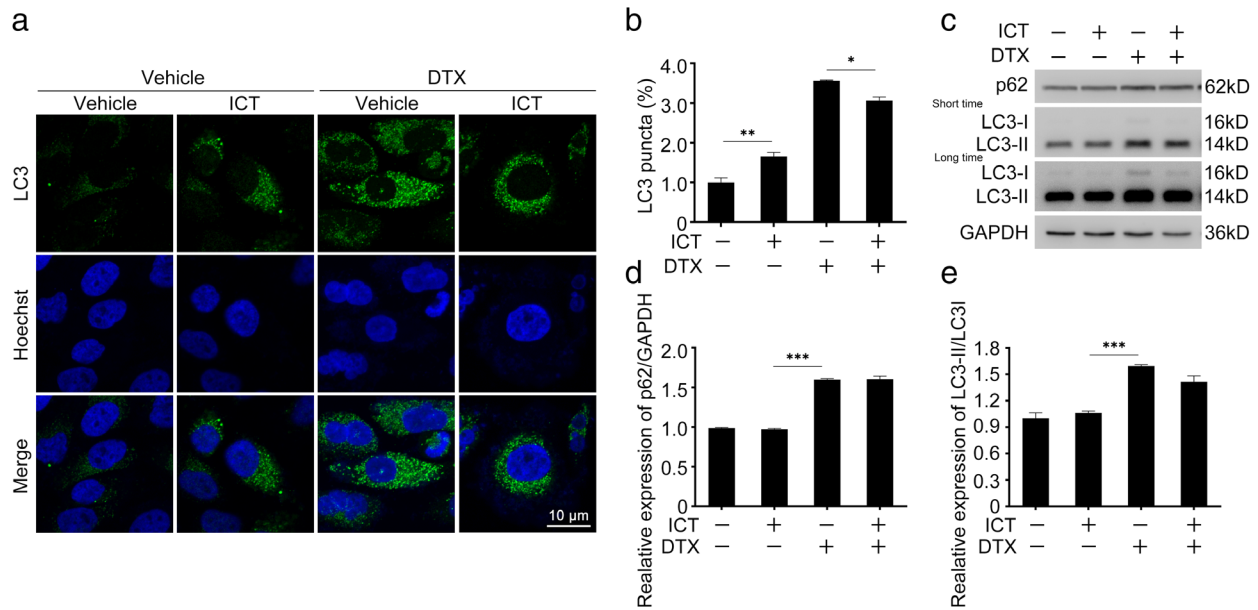


FIGURE 4 ICT inhibits the autophagy in HaCaT cells induced by DTX. HaCaT cells were induced with DTX (2.5 nM) for 48 h and then treated with ICT (10 μ M) for 24 h. (a, b) The LC3 puncta (green) and nucleus (blue) of HaCaT cells were detected by immunofluorescence and captured under confocal microscopy (scale bars = 10 μ m). (c–e) The expression of p62, LC3-I, and LC3-II of HaCaT cells was detected by western blotting. The relative ratio of p62/GAPDH and LC3II/LC3I was quantified. All data were expressed as the mean \pm SD from three independent experiments. *** p < 0.001; ** p < 0.01, * p < 0.05. ICT, icaritin; DTX, docetaxel; LC3, microtubule-associated protein 1A/1B-light chain 3; p62, the ubiquitin binding autophagy receptor protein

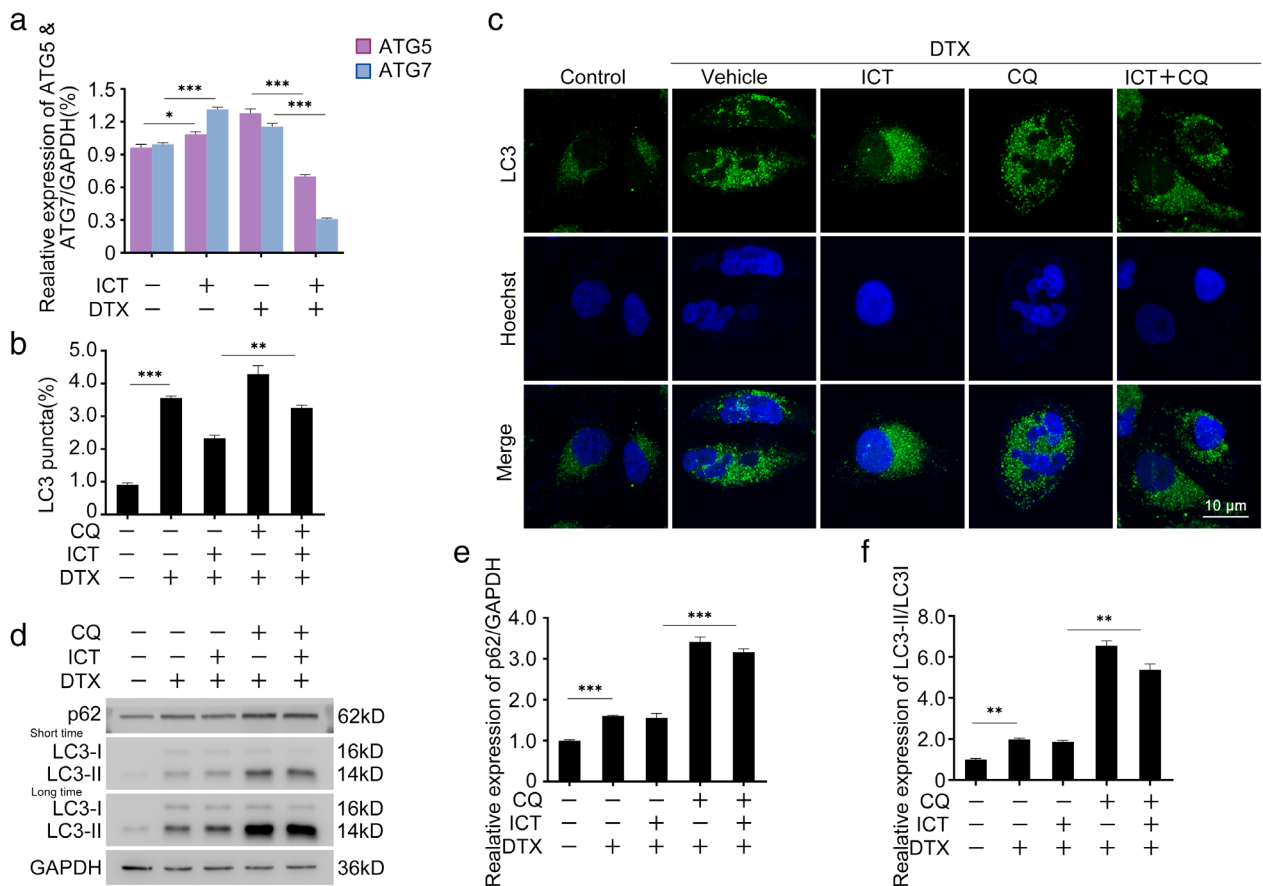


FIGURE 5 ICT blocks the autophagic flux of HaCaT cells induced by DTX. HaCaT cells were induced with DTX (2.5 nM) for 48 h and then treated with ICT (10 μ M) alone or in combination with CQ (10 μ M) for 24 h. (a) The relative ratio of ATG5/GAPDH and ATG7/GAPDH was quantified. (b, c) The LC3 puncta (green) and nucleus (blue) of HaCaT cells were determined by immunofluorescence and captured under confocal microscopy (scale bars = 10 μ m). LC3 puncta per cell was quantified. (d–f) The expression of p62, LC3-I, and LC3-II of HaCaT cells was measured by western blotting. The relative ratio of p62/GAPDH and LC3II/LC3I was quantified. All data were expressed as the mean \pm SD from three independent experiments. *** p < 0.001; ** p < 0.01. ICT, icaritin; DTX, docetaxel; ATG5, autophagy related 5; ATG7, autophagy related 7; GAPDH, glyceraldehyde 3-phosphate dehydrogenase; CQ, chloroquine; LC3, microtubule-associated protein 1A/1B-light chain 3; p62, the ubiquitin-binding autophagy receptor protein

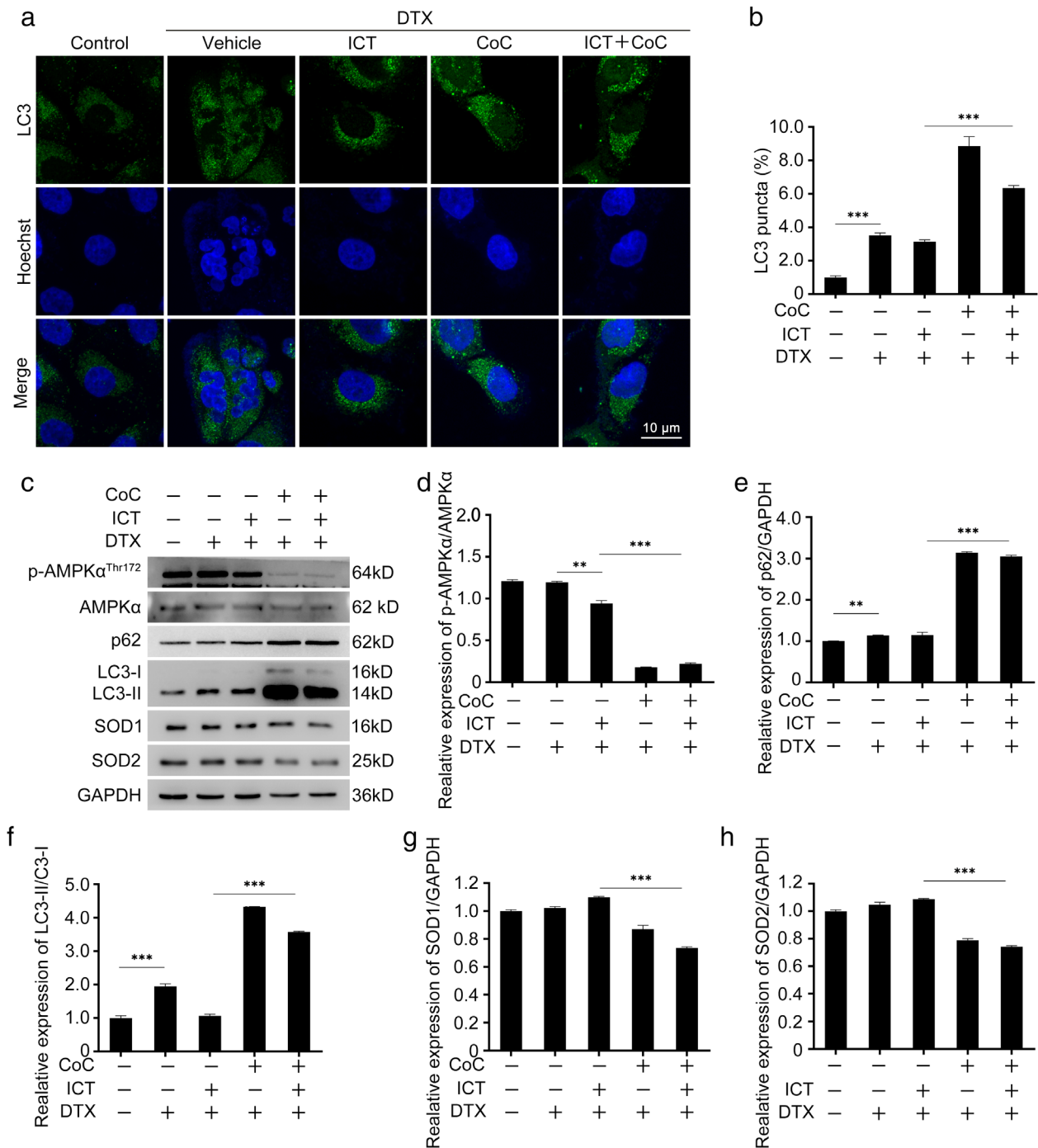


FIGURE 6 ICT regulates autophagy and ROS by activating AMPK in HaCaT cells induced by DTX. HaCaT cells were induced with DTX (2.5 nM) for 48 h and then treated with ICT (10 μ M) alone or in combination with CoC (10 μ M) for 24 h. (a, b) The LC3 puncta (green) and nucleus (blue) of HaCaT cells were determined by immunofluorescence and captured under confocal microscopy (scale bars = 10 μ m). (c–h) The expression of p-AMPK α , AMPK α , p62, LC3-I, LC3-II, SOD1, and SOD2 of HaCaT cells was measured by western blotting. The relative ratio of p-AMPK α /AMPK α , LC3II/LC3I, SOD1/GAPDH, and SOD2/GAPDH was quantified. All data were expressed as the mean \pm SD from three independent experiments. *** p < 0.001; ** p < 0.01. ICT, icaritin; DTX, docetaxel; p-AMPK α , phosphor-AMPK α (AMP-activated protein kinase α subunit); GAPDH, glyceraldehyde 3-phosphate dehydrogenase; CoC, compound C; LC3, microtubule-associated protein 1A/1B-light chain 3; p62, the ubiquitin-binding autophagy receptor protein; SOD1, superoxide dismutase type 1; SOD2, superoxide dismutase type 2

decreased ROS in DTX-induced HaCaT cells, which was reversed by TAM. ICT increased the expression of SOD1 and SOD2 in DTX-induced HaCaT cells, which was

reversed by TAM (Figure 7l–n). These results indicated that ICT regulates the phosphorylation of AMPK, autophagy, and ROS via ER.

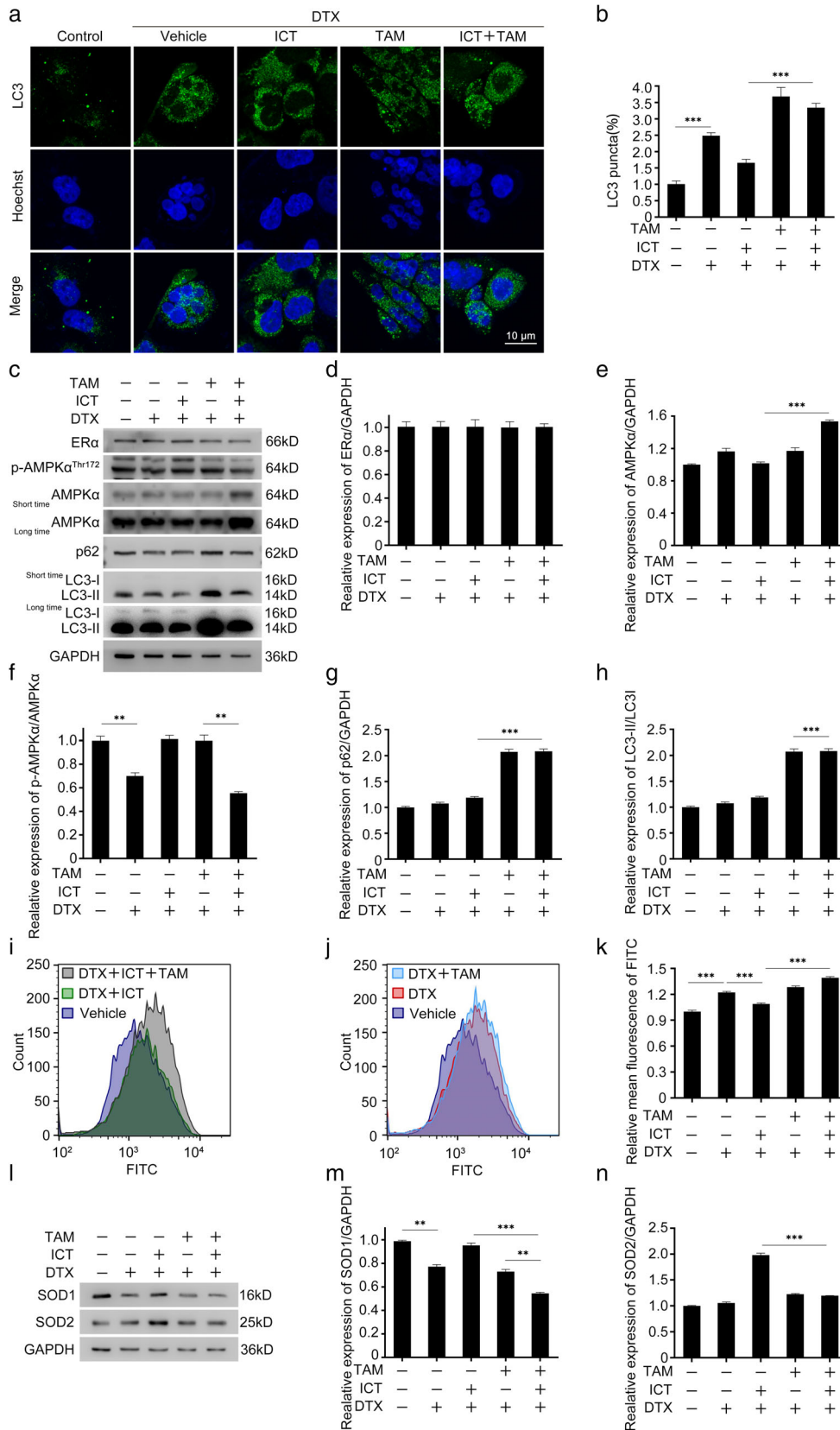


FIGURE 7 ICT regulates autophagy via ER in HaCaT cells induced by DTX. HaCaT cells were induced with DTX (2.5 nM) for 48 h and then treated with ICT (10 μM) alone or in combination with TAM (15 μM) for 24 h. (a, b) The LC3 puncta (green) and nucleus (blue) of HaCaT cells were detected by immunofluorescence and captured under confocal microscopy (scale bars = 10 μm). (c–h) The expression of ERα, AMPKα, p-AMPKα, p62, LC3-I and LC3-II in HaCaT cells was determined by western blotting. The relative ratio of ERα/GAPDH, AMPKα/GAPDH, p-AMPKα/AMPKα, p62/GAPDH, and LC3II/LC3I was quantified. (i–k) The ROS levels of HaCaT cells were measured by flow cytometry (FITC channel) after DHE staining. (l–n) The expression of SOD1 and SOD2 in HaCaT cells was detected by western blotting. The relative ratio of SOD1/GAPDH and SOD2/GAPDH was quantified. All data were expressed as the mean ± SD from three independent experiments. ****p* < 0.001. ICT, icaritin; DTX, docetaxel; TAM, tamoxifen; LC3, microtubule-associated protein 1A/1B-light chain 3; ERs, estrogen receptors; ERα, estrogen receptor alpha; AMPKα, AMP-activated protein kinase α subunit; p-AMPKα, phosphor-AMPKα; p62, the ubiquitin-binding autophagy receptor protein; GAPDH, glyceraldehyde 3-phosphate dehydrogenase; ROS, reactive oxygen species; DHE, dihydroethidium; SOD1, superoxide dismutase type 1; SOD2, superoxide dismutase type 2; NQO1, NAD(P)H: quinone oxidoreductase

DISCUSSION

Taxanes such as DTX are widely used for a variety of cancers, especially breast cancer.²⁶ Notably, more and more

cases of DTX extravasation-induced skin injury have been reported. When DTX leaks into soft tissue and induces necrosis of cells, serious complications may occur, including the macula, papules, lupus erythematosus, and other life-

threatening skin diseases, such as Stevens-Johnson syndrome, toxic epidermal necrolysis, and erythema multiforme. In addition, DTX induces recall inflammatory skin reactions such as skin pigment changes, edema, and sclerosis.²⁷ As recommended by the “Prevention and treatment of chemotherapy extravasation” of the group standard of the Chinese Nursing Society of China, hyaluronidase is used 1 h for taxane extravasation. Nonetheless, allergic reactions are a common side effect of hyaluronidase and therefore a skin test is compulsory before injection. In particular, hyaluronidase cannot be used in the case of local tissue infection, or the infection spreads. Therefore, finding an effective and safe medicine for DTX-induced skin injury is urgently required. Our study observed that ICT increases the viability and decreases apoptosis of DTX-induced HaCaT cells. Furthermore, the safety of ICT in the treatment of advanced hepatocellular carcinoma has been confirmed.²⁸ Importantly, as a compound with a molecular weight of 386.4, ICT can be administered in a number of dosage forms. The efficacy of ICT against advanced and breast cancer (NCT01278810) hepatocellular carcinoma (NCT01972672 and NCT03236649) is under evaluation by clinical trials. Therefore, ICT can alleviate DTX extravasation-induced skin injury with higher efficacy and safety compared with current measures. ICT may even be administered in combination with DTX to treat breast and other cancers. The evidence suggests that ICT is a promising candidate for DTX extravasation.

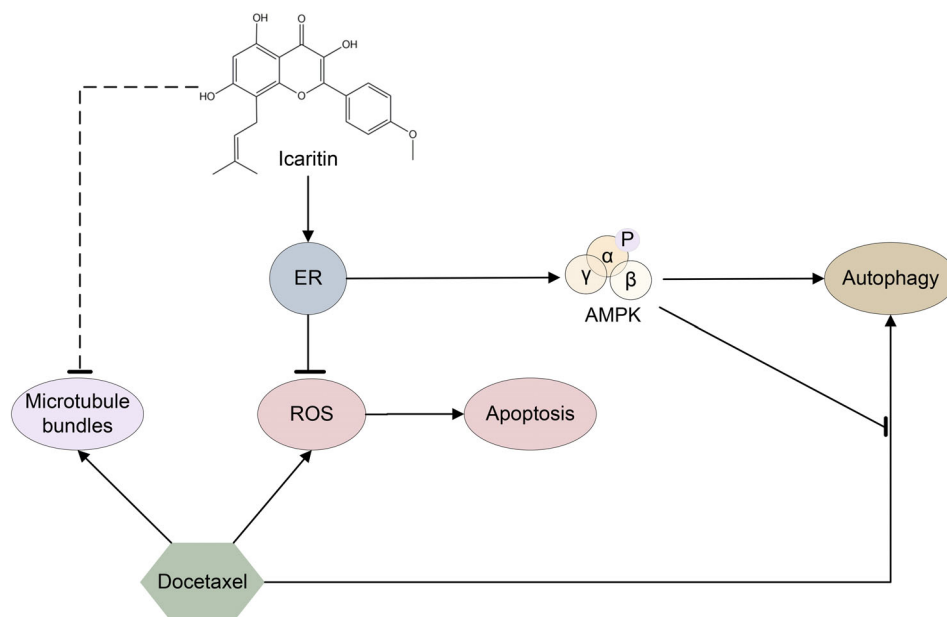
Taxanes interfere with cell mitosis by promoting the polymerization of microtubules and inhibiting cell proliferation.²⁹ Taxanes promote the polymerization of microtubules in normal skin cells and cause skin damage after extravasation. Our results confirmed that DTX does promote microtubule aggregation in HaCaT cells. In addition, studies have shown that many antitumor drugs cause mitochondrial regulation disorder by overactivating or inhibiting mitochondria,

thereby causing tumor cell apoptosis to play an antitumor effect.²⁹ We observed that DTX reduces the number of mitochondria in HaCaT cells, changes the karyotype, and accumulates ROS, which in turn affects cell viability and causes skin injury. Surprisingly, our study found that ICT promotes the depolymerization of microtubule bundles induced by DTX and restores cell morphology. We also observed that ICT increased the number of mitochondria of damaged cells and reduces the accumulation of ROS. All these results demonstrated that ICT alleviates DTX-induced skin injury by increasing the number of mitochondria and reducing ROS accumulation.

Autophagy, a type of programmed cell death besides apoptosis, participates in a variety of biological events like apoptosis, including maintaining cell morphology and tissue homeostasis.³⁰ Studies have shown that regulating autophagy alleviates skin photodamage and mechanical damage.^{31,32} Our results showed that DTX promotes the initiation of autophagy by increasing the expression of ATG5 and ATG7 in HaCaT cells. ICT also increases the number of autophagosomes, but inhibits the fusion of autophagosomes with lysosomes, that is, blocking the autophagic flow. Our present study demonstrated that ICT activates the initiation of autophagy in HaCaT cells, and blocks the autophagic flux in DTX-induced HaCaT cells. ICT reduces skin injury by inhibiting autophagy in DTX-induced HaCaT cells. Our previous study also demonstrated that ICT regulates autophagy depending on the cell status of 3 T3-L1 cells and C2C12 cells.³³

ICT has been reported to regulate autophagy via AMPK.^{14,33} ICT has also been reported to inhibit skin fibrosis by regulating AMPK and the Wnt/ β -catenin pathway.³⁴ We therefore assumed that ICT alleviates DTX-induced skin injury through activating AMPK. The AMPK inhibitor, CoC, blocked the effects of ICT on autophagy and the

FIGURE 8 ICT alleviates DTX-induced skin injury by reducing ROS via ERs. ICT alleviates DTX-induced skin injury by reducing ROS via ER, which in turn reduces microtubule bundles and autophagy. The solid line indicates that the mechanism is clear, while the dashed line indicates that the mechanism remains unclear



autophagic flux. More reports indicated that ICT exerts pharmacological effects by acting on ER.¹⁴ The ER modulator, TAM, was employed. We observed that TAM reversed the effect of ICT on autophagy and ROS accumulation, indicating that ICT plays effects via ER. Our results also proved that ICT does regulate autophagy and ROS levels by activating AMPK via ER. Moreover, we found that ICT did not play a role in changing the expression of ER. Our previous study also demonstrated that the effects of ICT on breast cancer cells depend on the status of ER.¹⁴ Therefore, it is reasonable to speculate that the estrogen-like effects of ICT depend largely on the status of the ER. This finding may influence the clinical application strategy of ICT.

Our study has several limitations. First, it was carried out on DTX-induced HaCaT cells, which should be further verified by animal experiments. Second, the mechanism of ICT on the depolymerization of microtubules remains unclear.

In summary, ICT alleviates DTX-induced skin injury by regulating autophagy and reducing ROS accumulation by activating AMPK via acting as an ER modulator. As shown in Figure 8, ICT alleviates DTX-induced skin injury by alleviating the microtubule bundles, but the specific mechanism is unknown. At the same time, ICT, as an ER modulator, promotes the phosphorylation of the α subunit of AMPK to activate AMPK, thereby regulating the level of autophagy. ICT also reduces the level of ROS by acting as an ER modulator to reduce cell apoptosis.

ACKNOWLEDGMENTS

We thank Professor Shuyu Zhang of Sichuan University for providing us with HaCaT cells. This study was financially supported by the National Natural Science Foundation of China (grant no. 81770580, 82170844).

CONFLICT OF INTEREST

The authors declare that there are no conflicts of interest.

ORCID

Yuan-Yuan Zhang  <https://orcid.org/0000-0002-9263-6262>

REFERENCES

- Ringel I, Horwitz SB. Studies with RP 56976 (taxotere): a semisynthetic analogue of taxol. *J Natl Cancer Inst.* 1991;83(4):288–91.
- Ashrafzadeh M, Ahmadi Z, Mohamadi N, Zarrabi A, Abasi S, Dehghannoudeh G, et al. Chitosan-based advanced materials for docetaxel and paclitaxel delivery: recent advances and future directions in cancer theranostics. *Int J Biol Macromol.* 2020;145:282–300.
- Lyseng-Williamson KA, Fenton C. Docetaxel: a review of its use in metastatic breast cancer. *Drugs.* 2005;65(17):2513–31.
- Cifuentes L, Ring J, Brockow K. Extravasation of docetaxel. *J Dtsch Dermatol Ges.* 2012;10(9):3.
- Weinhouse S. On respiratory impairment in cancer cells. *Science.* 1956;124(3215):267–9.
- Porporato PE, Filigheddu N, Pedro JMBS, Kroemer G, Galluzzi L. Mitochondrial metabolism and cancer. *Cell Res.* 2018;28(3):265–80.
- Sharma LK, Fang H, Liu J, Vartak R, Deng J, Bai Y. Mitochondrial respiratory complex I dysfunction promotes tumorigenesis through ROS alteration and AKT activation. *Hum Mol Genet.* 2011;20(23):4605–16.
- Rinnerthaler M, Bischof J, Streubel M, Trost A, Richter K. Oxidative stress in aging human skin. *Biomolecules.* 2015;5(2):545–89.
- Li L, Tan J, Miao Y, Lei P, Zhang Q. ROS and autophagy: interactions and molecular regulatory mechanisms. *Cell Mol Neurobiol.* 2015; 35(5):615–21.
- Kim J, Kundu M, Viollet B, Guan KL. AMPK and mTOR regulate autophagy through direct phosphorylation of Ulk1. *Nat Cell Biol.* 2011;13(2):132–41.
- Herzig S, Shaw RJ. AMPK: guardian of metabolism and mitochondrial homeostasis. *Nat Rev Mol Cell Biol.* 2018;19(2):121–35.
- Liu J, Ye H, Lou Y. Determination of rat urinary metabolites of icariin in vivo and estrogenic activities of its metabolites on MCF-7 cells. *Pharmazie.* 2005;60(2):120–5.
- Huang L, Wang X, Cao H, Li L, Chow DHK, Tian L, et al. A bone-targeting delivery system carrying osteogenic phytochemical icaritin prevents osteoporosis in mice. *Biomaterials.* 2018;182:58–71.
- Tao CC, Wu Y, Gao X, Qiao L, Yang Y, Li F, et al. The antitumor effects of icaritin against breast cancer is related to estrogen receptors. *Curr Mol Med.* 2021;21(1):73–85.
- Zhou C, Gu J, Zhang G, Dong D, Yang Q, Chen MB, et al. AMPK-autophagy inhibition sensitizes icaritin-induced anti-colorectal cancer cell activity. *Oncotarget.* 2017;8(9):14736–47.
- Vichai V, Kirtikara K. Sulforhodamine B colorimetric assay for cytotoxicity screening. *Nat Protoc.* 2006;1(3):1112–6.
- Tian X, Zhao L, Song X, Yan Y, Liu N, Li T, et al. HSP27 inhibits homocysteine-induced endothelial apoptosis by modulation of ROS production and mitochondrial caspase-dependent apoptotic pathway. *Biomed Res Int.* 2016;2016:4847874.
- Im K, Mareninov S, Diaz MF, Yong WH. An introduction to performing immunofluorescence staining. *Methods Mol Biol.* 2019;1897: 299–311.
- Wick SM, Duniec J. Immunofluorescence microscopy of tubulin and microtubule arrays in plant cells. I. Preprophase band development and concomitant appearance of nuclear envelope-associated tubulin. *J Cell Biol.* 1983;97(1):235–43.
- Mahmood T, Yang P-C. Western blot: technique, theory, and trouble shooting. *N Am J Med Sci.* 2012;4(9):429–34.
- Scorrano L, Petronilli V, Colonna R, di Lisa F, Bernardi P. Chloromethyltetramethylrosamine (Mitotracker Orange) induces the mitochondrial permeability transition and inhibits respiratory complex I. Implications for the mechanism of cytochrome c release. *J Biol Chem.* 1999;274(35):24657–63.
- Hubbert C, Guardiola A, Shao R, Kawaguchi Y, Ito A, Nixon A, et al. HDAC6 is a microtubule-associated deacetylase. *Nature.* 2002; 417(6887):455–8.
- Haggarty SJ, Koeller KM, Wong JC, Grozinger CM, Schreiber SL. Domain-selective small-molecule inhibitor of histone deacetylase 6 (HDAC6)-mediated tubulin deacetylation. *Proc Natl Acad Sci U S A.* 2003;100(8):4389–94.
- Vucicevic L, Misirkic M, Kristina J, Vilimanovich U, Sudar E, Isenovic E, et al. Compound C induces protective autophagy in cancer cells through AMPK inhibition-independent blockade of Akt/mTOR pathway. *Autophagy.* 2011;7(1):40–50.
- Zou Y, Wang Q, Li B, Xie B, Wang W. Temozolomide induces autophagy via ATM-AMPK-ULK1 pathways in glioma. *Mol Med Rep.* 2014;10(1):411–6.
- Shao Z, Pang D, Yang H, Li W, Wang S, Cui S, et al. Efficacy, safety, and tolerability of pertuzumab, trastuzumab, and docetaxel for patients with early or locally advanced ERBB2-positive breast cancer in Asia: The PEONY phase 3 randomized clinical trial. *JAMA Oncol.* 2020;6(3):e193692.
- Sibaud V, Lebœuf NR, Roche H, Belum VR, Gladieff L, Deslandres M, et al. Dermatological adverse events with taxane chemotherapy. *Eur J Dermatol.* 2016;26(5):427–43.
- Fan Y, Li S, Ding X, Yue J, Jiang J, Zhao H, et al. First-in-class immune-modulating small molecule Icaritin in advanced hepatocellular carcinoma: preliminary results of safety, durable survival and immune biomarkers. *BMC Cancer.* 2019;19(1):279.

29. Mukhtar E, Adhami VM, Mukhtar H. Targeting microtubules by natural agents for cancer therapy. *Mol Cancer Ther.* 2014;13(2):275–84.
30. Tsujimoto Y, Shimizu S. Another way to die: autophagic programmed cell death. *Cell Death Differ.* 2005;12(Suppl 2):1528–34.
31. Hao D, Wen X, Liu L, Wang L, Zhou X, Li Y, et al. Sanshool improves UVB-induced skin photodamage by targeting JAK2/STAT3-dependent autophagy. *Cell Death Dis.* 2019;10(1):19.
32. Kimura A, Ishida Y, Nosaka M, Shiraki M, Hama M, Kawaguchi T, et al. Autophagy in skin wounds: a novel marker for vital reactions. *Int J Leg Med.* 2015;129(3):537–41.
33. Wu Y, Yang Y, Li F, Zou J, Wang YH, Xu MX, et al. Icaritin attenuates lipid accumulation by increasing energy expenditure and autophagy regulated by phosphorylating AMPK. *J Clin Transl Hepatol.* 2021;9(3):373–83.
34. Li M, Liu Q, He S, Kong X, Lin J, Huang Y, et al. Icaritin inhibits skin fibrosis through regulating AMPK and Wnt/ β -catenin signaling. *Cell Biochem Biophys.* 2021;79(2):231–8.

How to cite this article: Zou J, Xu M-X, Li F, Wang Y-H, Li X-Q, Yu D-J, et al. Icaritin alleviates docetaxel-induced skin injury by suppressing reactive oxygen species via estrogen receptors. *Thorac Cancer.* 2022;13:190–201. <https://doi.org/10.1111/1759-7714.14245>